Multi-Objective Kriging-Based Optimization For Impeller Centrifugal Compressor

Muhamad Jayadi[1*], Pramudita Satria Palar[1], Yohanes Bimo Dwianto[1]

{jayadimuhamad72@gmail.com[1], pramsp@itb.ac.id[1], bimo@itb.ac.id[1] }

[1] Bandung Institute of Technology, Jl. Ganesha No. 10, Bandung, West Java, Indonesia

Abstract. The centrifugal compressor consists of several parts: an Impeller, Diffuser, and inlet guide Vanes (IGV). The compressor has two important parameters: Pressure Ratio and Efficiency. Enhancing one of these parameters will lessen the performance of the opposite parameter. The impeller has continuously stepped forward and been redesigned to acquire great performance. The main blade's leading edge design is of primary importance. Several approaches and methods have been developed to increase centrifugal compressor performance. This research will concentrate on multi-objective optimization to increase the overall performance of the SRV2-O centrifugal compressor's impeller by deforming it. The optimization process was done by evaluating the goal function using the Kriging-surrogate Model based on Expected Hypervolume Improvement and Computational Fluid Dynamics. The impeller will be optimized by two variables using the control point of Bezier curve. The optimization approaches produced multiple correct answers known as the Pareto front. From the results, this approach increases the pressure ratio by 1.33% and the efficiency by 5.22%. Furthermore, the shock wave intensity at the leading edge is reduced, and flow separation towards the trailing edge is eliminated.

Keywords: Centrifugal compressor, impeller, multi-objective optimization, Kriging, EHVI

1 Introduction

A centrifugal compressor is made up of various components Impeller, Diffuser, and inlet guide Vanes (IGV). The centrifugal compressor component as shown in Fig. 1 There are two important parameters in the compressor, namely Pressure Ratio and Efficiency. Both parameters are opposite. Enhancing one of these parameters will lessen the performance of the opposite parameter. One of the most significant components of centrifugal compressors is the impeller. The impeller provides kinetic energy to the air and converts the velocity of the air into pressure in the diffuser [1]. Rapidly revolving impeller blades push fluid through the impeller. The fluid velocity is converted to pressure, partially in the impeller and partially in the stationary diffusers since it plays an important role in fluid dynamics. The impeller is continuously has been stepped

AVINER 2023, November 08-09, Jakarta, Indonesia

DOI 10.4108/eai.8-11-2023.2345844

forward and redesigned to acquire great performance. However, centrifugal impellers have several restrictions that must be addressed via design. The compressor impeller's blades have always had the greatest influence on the efficiency and performance of these machine parts. The design of the main blade leading edge is critical in centrifugal compressors because it increases the efficiency of the impeller stage [2]. When the compressor blade's leading-edge sweeps forward, the tip area transmits shock even more to the suction side. So, tip shock decreases and increases compressor performance, particularly isentropic efficiency. By reducing the size of the splitter blade and putting it along the meridional length of the main blade, efficiency and operating range are improved [2].

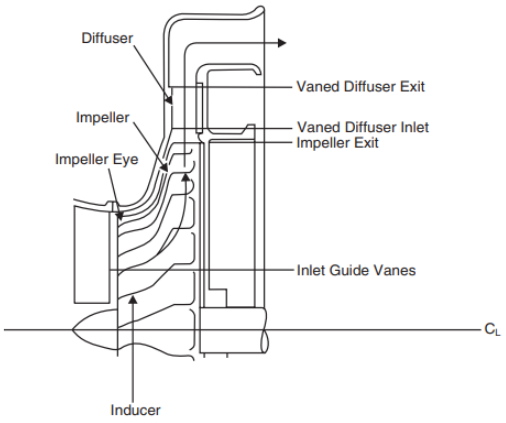

Fig. 1. Centrifugal Compressor Components [1]

The primary goal has been the optimization design of centrifugal compressors with high pressure ratios and efficiency. There are several methods and algorithms that have been created to produce optimal designs based on initial design circumstances. [3]. On the hub curve control line, an optimization approach was used, and the results revealed that the optimum locations enhanced efficiency by 2.5% and pressure ratio by 7.28%. Variations in blade angle, Bezier curve at the leading edge of the blade, and thickness curve at hub and shroud all improved the centrifugal compressor's efficiency and pressure ratio. [4]. Several researchers have used Bezier curves to optimize the blade profile. For the multi-objective optimization of pressure ratio and efficiency for an impeller, Benini [5] determined the blade profile by Bezier curve parameters. Samad and Kim [6] used a surrogate model to optimize the stacking line and thickness of the compressor blade using the Bezier curve. Several approaches and methods have been used to increase centrifugal compressor performance. Kim et al. [6] effectively improved the efficiency of a centrifugal compressor by 1.0% using the Radial Basis Neural Network approach by adjusting the contours of the impeller hub and shroud. Faza[7] published work on expected hypervolume improvement (EHVI) as the Kriging infill criterion for multi-objective optimization. In turbomachinery applications, a Study about surrogate-based optimization on the axial compressor has been conducted by Cahya [8].

This study will focus on the multi-objective optimization of SRV2-O centrifugal compressors by modifying their shape, hence enhancing the overall performance of the impeller. The SRV2-O was a Centrifugal compressor designed by DLR (German Aerospace Center). This compressor had characteristics of high-speed, high-pressure ratio, and mass flow. The SRV2-O geometry as shown in Fig.2

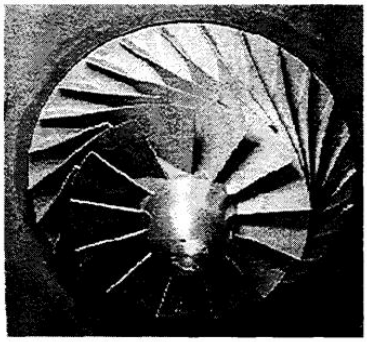

Fig. 2. SRV2-O Geometry

The findings of the compressor experiment design speed (50,000 1/min) and design mass flow rate (2.55kg/s) [9] shown in Fig.3. The impeller is made up of 13 complete and 13 splitter blades. The leading edges of splitter blades are 26% of the whole blade chord. The test case compressor has an outlet diameter of 112 mm and a tip speed of 586 m/s at 50000 1/min. Following the impeller is a vaneless diffuser. specification of SRV2-O centrifugal compressor is shown in Table 1[10].

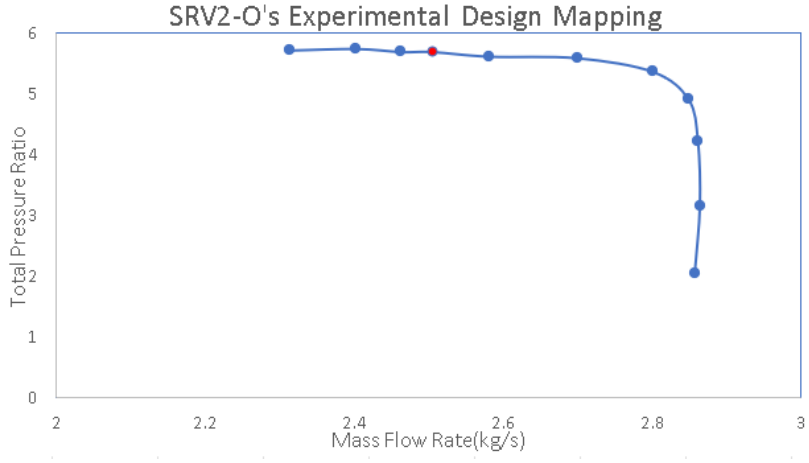

Fig. 3. Experimental Design Performance Map

Table 1. SRV2-O centrifugal compressor [10]

Parameters	Values
Inlet total pressure	101325 Pa
Inlet total temperature	288.15 K
Shaft speed	50000 rpm
Design mass flow rate	2.55 kg/s
Design mass flow rate	13/13
Leading Edge hub radius	30 mm
LE tip radius	78 mm
Blade angle LE tip	26.5 deg
Rel. Ma number tip inlet	1.3
Impeller tip radius	112 mm
Exit blade height	10.2 mm
Blade angle TE	52 deg
Impeller tip speed	586 m/s
Impeller pressure ratio	6.1
Efficiency	0.84

This study's optimization strategy attempts to get the most both namely the total pressure ratio and efficiency termed as multi-objective optimization. The optimization process uses the kriging-Surrogate Model based on Expected Hypervolume Improvement and computational fluid dynamics (CFD) for evaluating the objective function. The output of this optimization is a group of non-dominated optimum solutions (Pareto optimum).

2 Optimization Methodology

2.1 Objective Function and Design Variables

The centrifugal compressor's performance is evaluated using performance measures such as Isentropic Efficiency and Pressure Ratio. Pressure Ratio and Isentrofic Efficiency are objective functions in this work. from. The pressure ratio is evaluated using the below equation [11]:

$$\pi_c = \frac{P_{t4}}{P_{t1}} \tag{1}$$

Where P_{t4} is the pressure at the diffuser outlet, P_{t1} is the pressure at the inlet of compressor, and π_c stands total pressure ratio. Total to total isentropic efficiency can be found us with π_c found the above equation [11]:

$$\eta = \frac{\pi_c^{\frac{\gamma-1}{\gamma}} - 1}{\tau_c - 1} \quad (1)$$

Where η is total-to-total isentropic efficiency, and τ_c is temperature ratio.

In the present 3D CFD design optimization, geometric variables related to the shroud and hub forms of the impeller are employed as design variables. To define the splitters regarding the constant relative meridional location of the splitter leading edge, the camber curve of the main blade is shortened. As a result, when primary blades are modified, splitters will be adjusted similarly. The camber curves of the primary blade are built in the (m',θ) plane. Any of the curves is specified as a Bezier curve with eight control points. A polynomial curve of degree n is a Bézier curve of degree n. The primary advantage of defining contours with a Bezier curve is that the curves may be controlled by a small number of control points. Bézier curves provide systematic handling of curves, resulting in smooth curves with continuous derivatives. [12]. The Bernstein polynomials define a Bezier curve of rank n as follows.:

$$P(t) = \sum_{i=0}^{n} c_i B_i^i(t) \quad (2)$$

Theta angles of the front two control points at shroud sections (TS1 and TS2) are chosen as design variables, while others stay fixed. Fig.4 shows an illustration presenting the definition of camber curves.

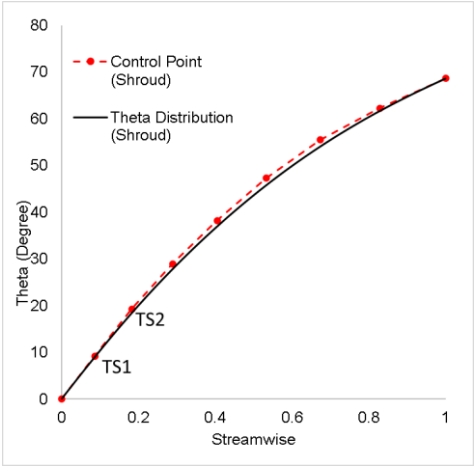

Fig. 4. Illustration Design Variables

2.2 Kriging Surrogate Model Based on Optimization

Optimization is the procedure of selecting the satisfactory viable choice or making something as fully perfect, functional, or optimum. Multi-objective optimization refers to the optimization of multiple conflicting objectives simultaneously. The purpose of multi-objective optimization is to discover solutions that are equally excellent for all

objectives, with different trade-offs called Pareto front or Pareto Optimal Solution or non-dominated Solutions.

The surrogate model is an engineering strategy for predicting the outcomes of a system or operation that resides in a black box or where the desired outcomes are difficult to get. Surrogate models are used for obtaining output values. $y^{(1)}, y^{(2)}, \ldots . y^{(n)}$, the result from a set of input $X^{(1)}, X^{(2)}, \ldots . X^{(n)}$ and find a best guess $\hat{f}(x)$ based on these known data, for displaying from real function [13]. Kriging is one of the surrogate models to map function developed by Danie G. Krige in 1951. This Model is a very flexible approximation model and can predict more accurately by making variations of θ and p. To predict the outcome of a black box, Kriging employs the basis function shown in equation 4. θ = variable modeling and p = correlation of each x.

$$\psi^{(i)} = \exp\left(-\sum_{j=1}^{k} \theta_j \left|x_j^{(i)} - x_j\right|^{p_j}\right) \tag{3}$$

The Optimization technique is shown in Fig. 5. Design Experiment is the first step in the Optimization procedure. In this step is to determine the input variables and output variables as objective functions that are material for optimization which becomes the initial design. The following steps is Computational Analysis has a goal to calculate the objective function for each initial design that will be initial samples using CFD, namely with Ansys CFX software. An initial sample is required for this stage, namely the construct surrogate model stage. In this stage, a sampling plan is needed as part of the initial sample. The main purpose of a sampling plan is to obtain a representative sample from the population that accurately reflects its characteristics. In the context of optimization, a sampling plan as space-filling refers to a strategy for selecting sample points that effectively cover and explore the entire search space to find an optimal solution. There are several methods and algorithms for creating space-filling sampling plans, some of which include Latin Hypercube Sampling, Sobol Sequence, and Halton Sequence. The optimization processes this time using Halton sampling plan. Halton Sampling Plan or Halton sequence uses the coprime number as a basis. It will generate a quasi-random sequence that spreads in a design space evenly. Although these sequences are predictable, they have a low discrepancy, which makes them look random in many situations. They were originally used in 1960 and are a type of quasi-random number sequence [14]. The advantages of this method are Leveling the sample, efficiency, and systematical information.

Determine a New Sample Point. The multi-objective Expected Hyper Volume Improvement (EHVI) is used to determine the updated sample. Expected Hypervolume Improvement (EHVI) is an infill criterion used in multi-objective optimization to guide the selection of candidate solutions for evaluating the objective functions. It is described as [15]

$$\text{EHVI}\ (\boldsymbol{\mu}, \boldsymbol{\sigma}, \boldsymbol{P}, \mathbf{r}) := \int_{\mathbb{R}^d} HVI(\mathcal{P}, \mathbf{y}) \cdot \text{PDF}_{\mu,\sigma}\ (\mathbf{y}) d\mathbf{y} \tag{4}$$

Where $PDF_{\mu,\sigma}$ is mean value distribution's multivariate independent normal distribution. $\mu \in \mathbb{R}^d$, and standard deviations $\sigma \in \mathbb{R}_+^d$ and Given parameters of the

multivariate predictive distribution $\boldsymbol{\mu}$, $\boldsymbol{\sigma}$ and the Pareto front approximation $\mathcal{P}$ the Expected hypervolume improvement (EHVI). EHVI shown in Fig. 5[15]

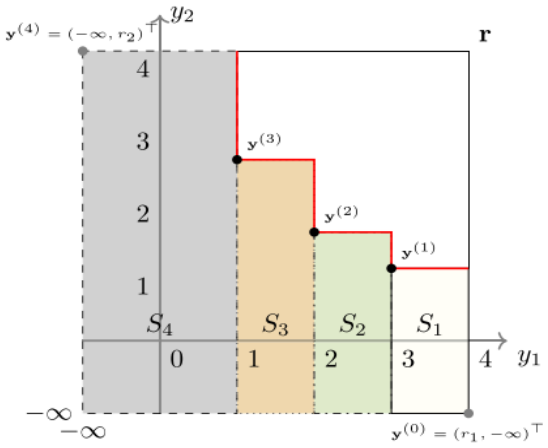

Fig. 5. Expected hypervolume improvement (EHVI)[15]

The following steps are Computational Analysis. This step is to Analyze the objective functions of the new samples. Looping Step for recreating surrogate model using all initial samples and updated samples and stopped at n-samples until finding the optimal point.

3 Computational Fluid Dynamics Setup

Computational Fluid Dynamics (CFD) is used for calculating Objective Functions. CFD Simulation is done using Ansys software. The simulation stage starts with creating the geometry using BladeGen. Next, generating meshing using TurboGrid and the last Solved using Ansys CFX. The geometry used in this simulation is the geometry centrifugal compressor SRV2-O. At this stage, several related parameters are given to build geometry such as Theta Angle Distribution, Blade Thickness, and Meridional Geometry Coordinate. The geometry results from BladeGen shown in Fig.6.

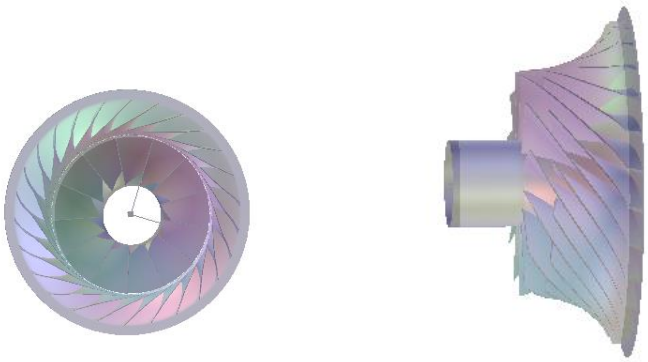

Fig. 6. SRV2-O's 3D Geometry in BladeGen

TurboGrid is a turbomachinery meshing method. The meshing process is due automatically with H-Grid Topology. The Automatic Method for the Singer Splitter centrifugal compressor was used for creating the mesh. This method will automatically select, depending on blade type (cut-off or rounded edges) and blade angles, the suitable topology. The result of the Meshing Show in Fig.7. The mesh size was controlled by the Global Size Factor Method with size Factor 1.8. To find out the right number of meshes, it is necessary to conduct a mesh independence test. The independence results are shown in Figure 9. The total element used from the Independency test result are 1,114,654 elements and 1,137,032 nodes. The quality of this mesh can be qualified as good mesh because in the Mesh Analysis menu, the percentage of" Bad" meshes is 0 percent for all criteria as shown in Fig.8.

.

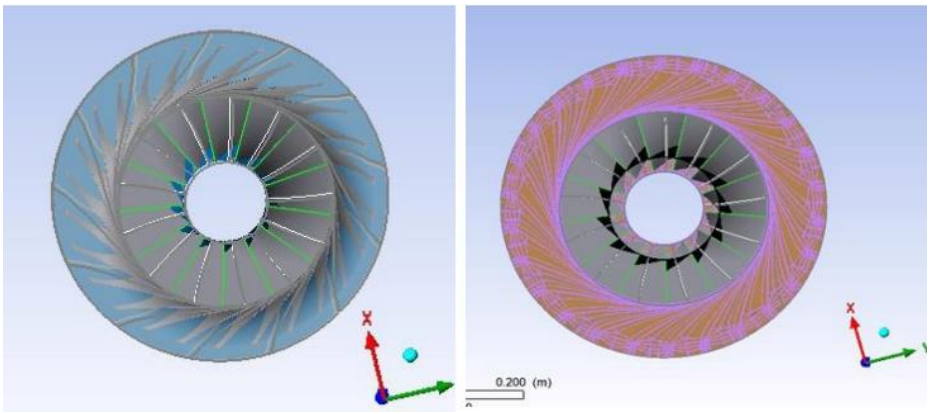

Fig. 7. SRV2-O Pre-Mesh(left) and Post mesh(right)

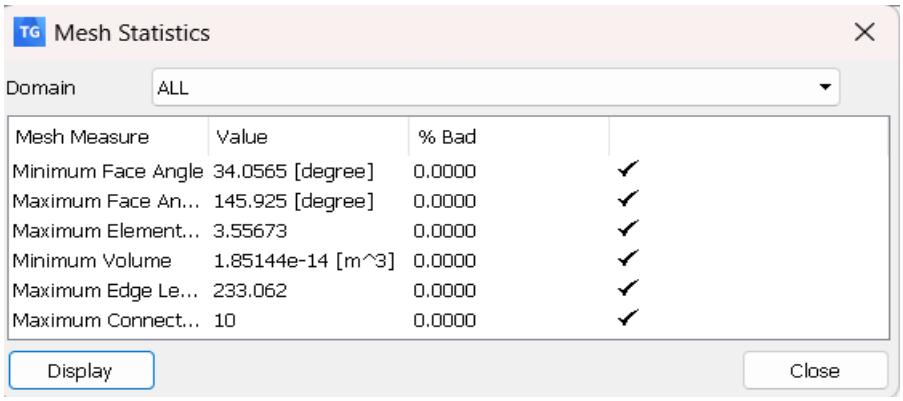

Fig. 8. SRV2-O Mesh Statistic

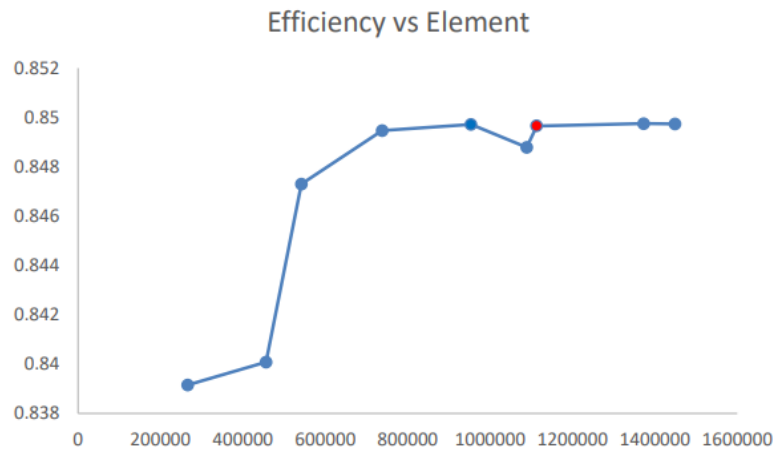

Fig. 9. SRV2-O Independency Mesh

The Problem was solved by ANSYS-CFX. The simulation setting with rotation speed of 50,000 RPM. The Turbulent model was chosen Shear Stress Transport model. The total pressure was 101.325 kPa and the temperature was 288.15. The impeller inlet boundary conditions were provided, and the static pressure was 350 kPa. The high-resolution approach is used for the solver settings, and the convergence residuals are set to 1E-5. The set-up simulation is shown in Fig.9. at below.

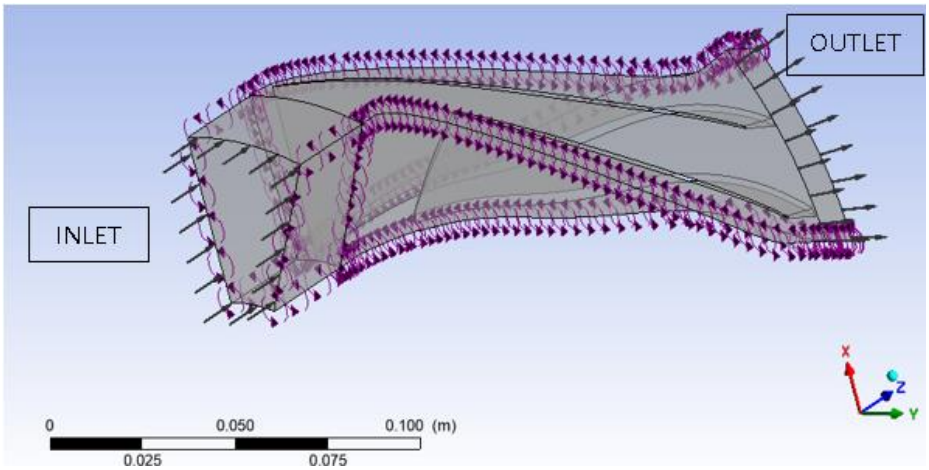

Fig. 9. Set-up Simulation

4 Result and Analysis

4.1 Computational Simulation Validation

The accuracy and validity of the simulation approach were tested by considering the findings of a previously published study and experimental and Computational results. The validation is performed at the shaft speed of 50,000 RPM. Figure 10 and Figure 11 illustrate pressure ratio and efficient isentropic variations normalized with mass flow rate at choke conditions, respectively.

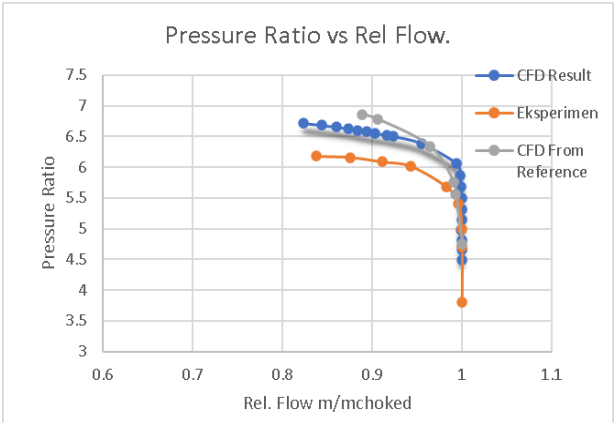

Fig. 10. Pressure Ratio versus normalized mass flow comparison

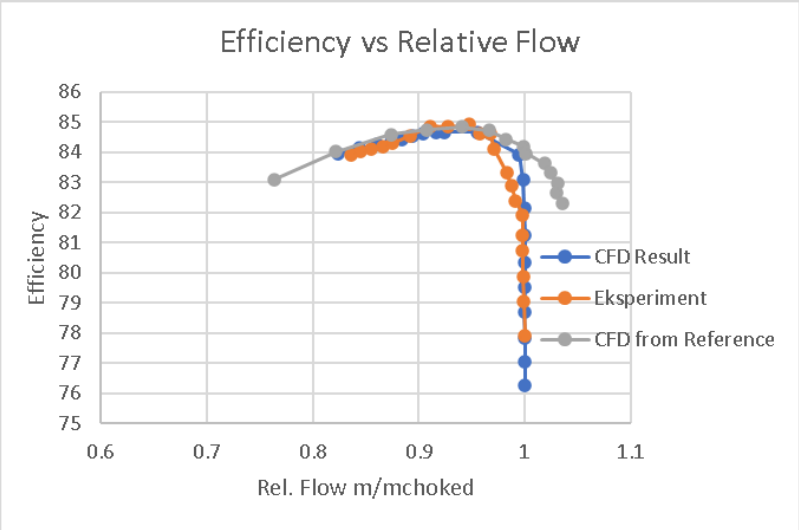

Fig. 11. Insetropic Efficiency versus normalized Massflow comparison

The Choke Masflow for computational result and experiment were 2.68 kg/s and 2.55 kg/s. From Fig.10. Pressure ratio yields an Error of around 9.03% and is still acceptable because it is under 10% from references. If compared with Computational references error of pressure ratio yields 6.71%. Besides, Fig.11. for Isentropic Efficiency comparing with experiment and Computational references the results of error 0.26% and 0.3%. An overview of the comparative analysis the outcome is shown in Table 2 below.

Table 2. Summarize Comparison

	Pressure Ratio	Efficiency	Mass Flow,kg/s
Experiment	5.65	0.8296	2.55
CFD Ref.	5.76	0.8474	2.81
Present	6.16066	0.831812	2.72

4.2 Two Variables Optimization

The optimization started with two design variables, namely TS1 and TS2. These design variables were chosen after a study on several works which shows that the tip of the leading edge of the impellers has a considerable impact on the compressor's performance [16]. TS1 and TS2 are Theta angle distributions at the shroud and as a control point in the Bezier curve. The first step in this optimization was to generate an initial

sampling plan. Initial sampling plan generated by Halton Sequences as space-filling. Halton Sequences needed Upper and Lower Boundary to generate this sampling and Range. For this research, the upper and Lower Boundary and Range are shown in Table 3. The initial sample was 20 samples.

Table 3. Two Variables Optimization Halton sequence Boundary

	Baseline°	Range °	Upper Boundary°	Lower Boundary°
TS1	9.230751	+-5	14.230751	4.230751
TS2	19.27785		24.27785	14.27785

An Updated Sample will add to the design space by utilizing Expected Hypervolume Improvement (EHVI) and the non-dominated solution or Pareto front obtained from the objective space. The objectives are calculated using ANSYS. The result of two variable optimizations is shown in Table 4

Table 4. Objective Two Variable optimization

	TS1	TS2	Pressure Ratio	Efficiency
Baseline	9.230751	19.277853	6.16066	0.831812
PRMAX	4.230751	14.27785	6.2437	0.8031
EFFMAX	12.35575	21.31488704	6.0954	0.8777

Table 4 shows that PRMAX as Maximal Pressure Ratio increases around 1.33% from baseline, in opposite directions decreases the efficiency by 3.57%. Efficiency is different from the pressure ratio, EFFMAX as maximum Efficiency has a better increase namely around 5.22% from baseline, and opposite direction the pressure ratio decreases by 1.07%. The Pareto Front Show in Fig.12

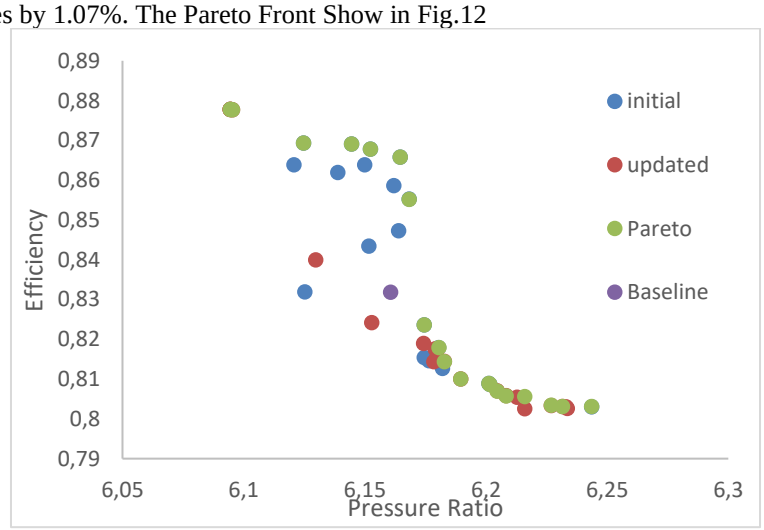

Fig. 12. Objective Space All samples

Figure 12 shows the entire objective space consisting of the baseline design. The initial sample is represented by initial. The improved result using optimization is represented by updated, and Pareto is the set of solutions given. Figure 12 also shows the optimization work is good enough to explore the objective space from the highest efficiency to the lowest and for the pressure ratio. This figure shows the maxima optimization. The Pareto front is good enough to predict Fig.13. Show Design variable comparing baseline with Optimized.

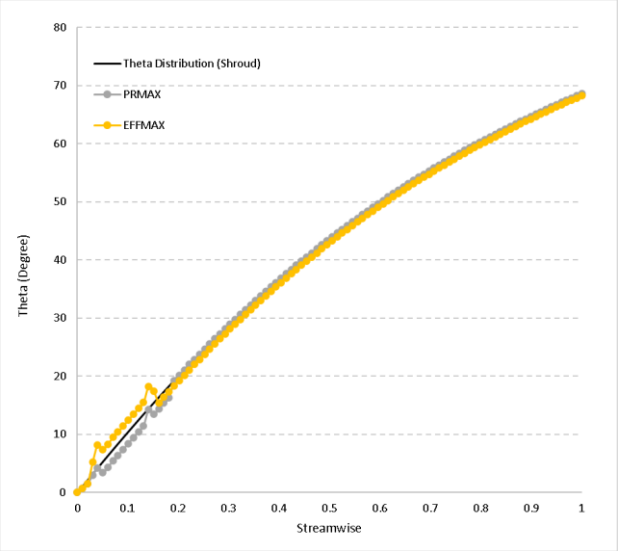

Fig. 13. Optimum Design Variable comparing baseline.

4.3 Flow Analysis

In this section, the post-processing results from CFD will be analyzed to acquire more knowledge of the relationship between each objective and the physical behavior of the flow of each result obtained by the optimization process of the SRV2-O centrifugal compressor. This study will be focused on the Mach number contour, static pressure contour of the meridional surface, and blade at 90% Span. Fig.14. illustrates the contour of the Static Pressure Ratio and Mach Number in the meridional profile for every design. The designs that have a high-pressure ratio PRMAX but lower in efficiency tend to have a region of low Mach number near the shroud of the impeller, indicating that the flow is separated from the blade. However, designs with high-efficiency EFFMAX have a smaller region of low Mach number, even EFFMAX the separation area is small, so the efficiency becomes the highest among all the designs. However, for static pressure contour in the meridional plane, there is no significant difference between every design.

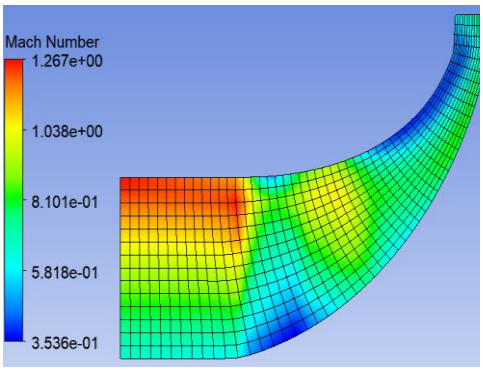

(a) Baseline

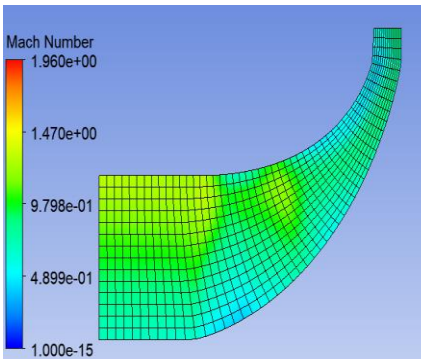

(b) EFFMAX

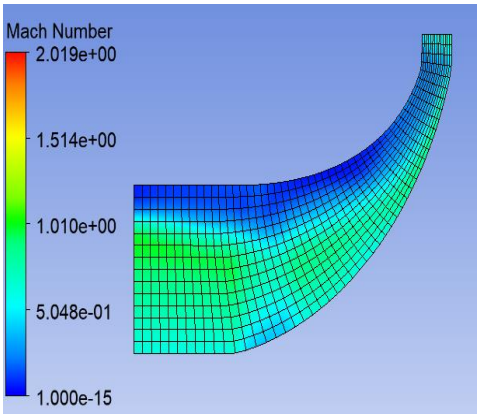

(c) PRMAX

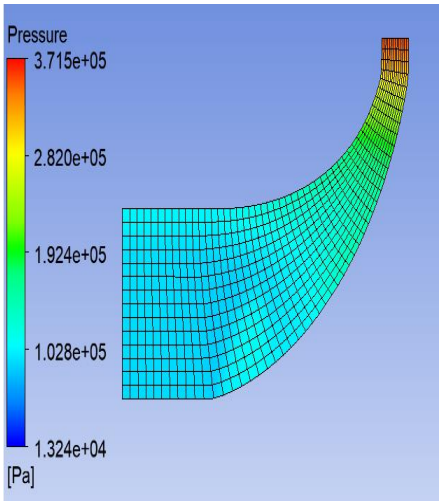

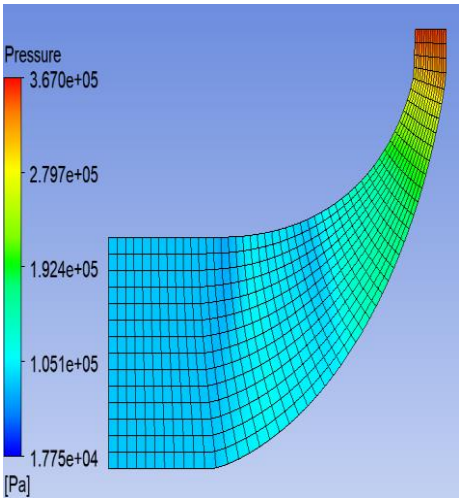

(d) PRMAX (e) EFFMAX

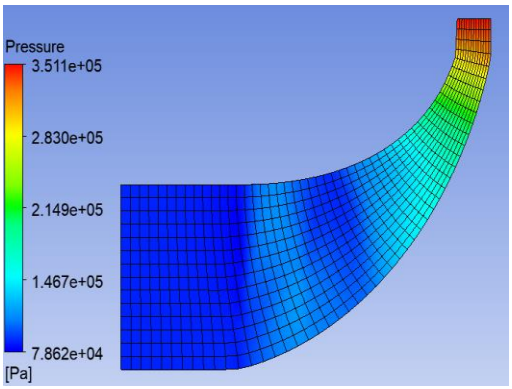

(f) Baseline

Fig. 14. Meridional Mach Number and Static Pressure Contour

Fig.14 Illustrates the contour of Mach Number and Static Pressure in Balde to Blade View for every design. Relative Mach Number distribution for 90% Span is seen in this image. In the instance of the baseline design centrifugal compressor depicted on the blade-to-blade surface, the Mach number at the blade leading edge seems to be greater than one around the stall and design point, but at the choke point, the Mach number switches to the compressor blade trailing edge. The greatest Mach number measured is roughly 2.09 at the impeller outflow at the choke point, which is completely different from the performance at the baseline. Besides, at 90% span, almost all the designs have massive separation regions except for one design that has the highest efficiency. For EFFMAX design shock in the leading edge reduces the strength of the shock to oblique shock which is weaker than the bow shock. In opposite, in designs that have a high-pressure ratio with low efficiency, the shock is strong and occurs even further at the inlet. Thus, separated flow occurs in all the areas of the impeller.

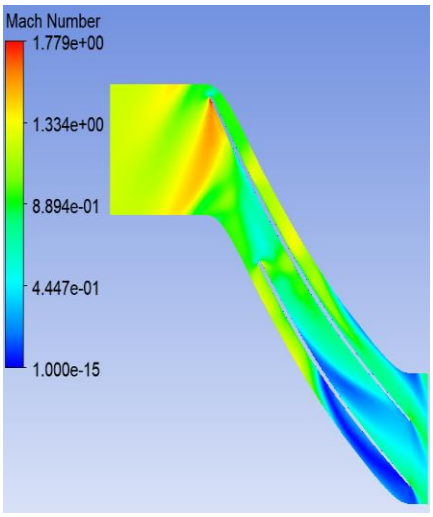

(a) BASELINE

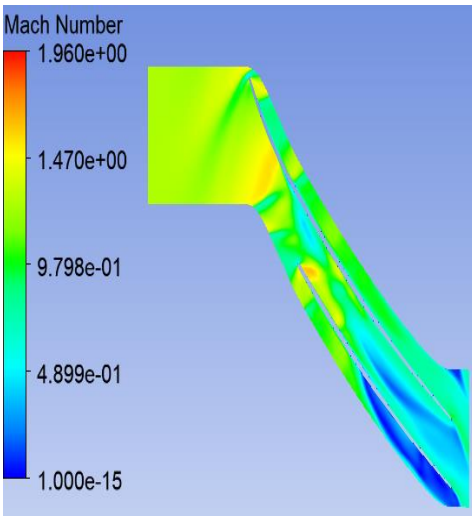

(b) EFFMAX

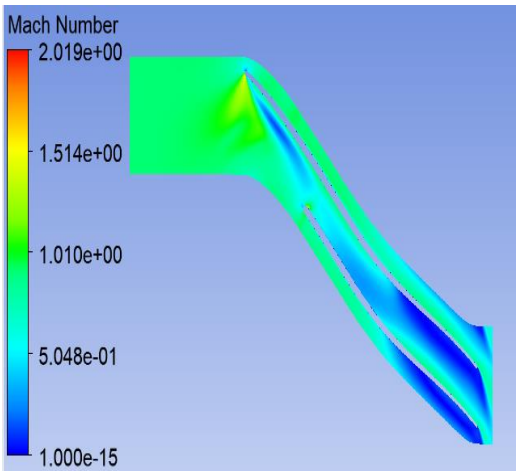

(c) PRMAX

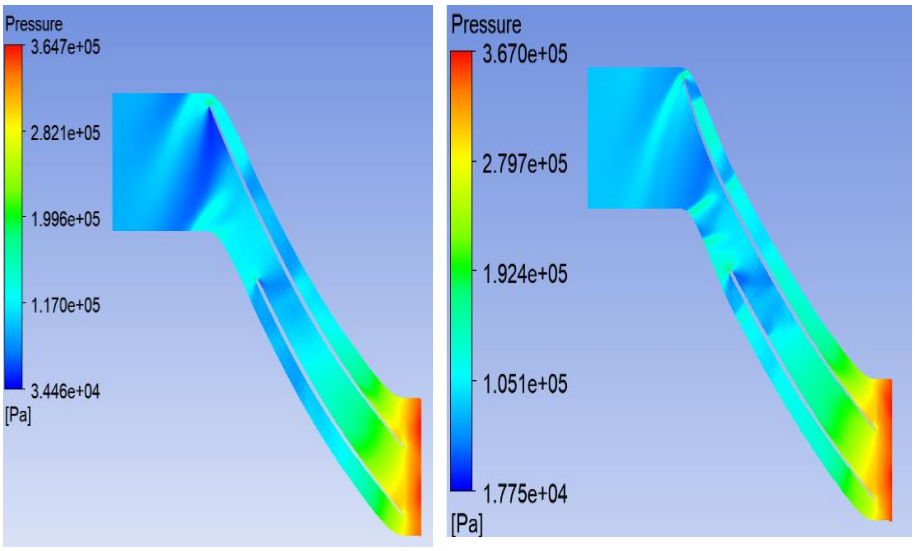

(d) BASELINE (e) EFFMAX

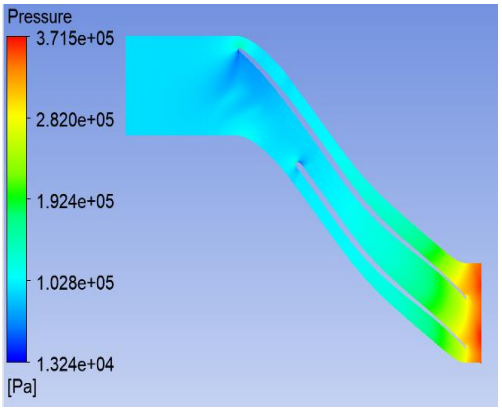

(f) PRMAX

Fig. 15. Blade to Blade Static Pressure and Mach Number Contour

5 Conclusion

The multi-objective optimization of the Kriging surrogate model has been done. The objective optimization namely pressure ratio and isentropic efficiency successfully obtained with a pareto front solution and optimum design. The EHVI as the infill criterion shows good results predicting the expected improvement of the objectives and supports adding new samples to the surrogate model. Two variable optimizations show good enough results for optimizing the objective. That is improving two objectives namely

pressure ratio and isentropic efficiency. The highest improvement is the Pressure Ratio increases around 1.33% and Efficiency has a better increase of around 5.22%.

References

1. Boyce, M., Gas Turbine Engineering Handbook.Third Edition. Gulf Professional Pub./Elsevier, Boston (2006)
2. F. Ghigliazza, A. Traverso, M. L. Ferrari, and J. Wingate, "Gt2008-50562," Asme Gt, pp. 1–9, (2008).
3. Tüchler S, Chen Z, Copeland CD. Multipoint shape optimization of an automotive radial compressor using a coupled computational fluid dynamics and genetic algorithm approach [J]. Energy; 165:543 (2018)
4. T. Raitor, O. Reutter, M. Aulich, and E. Nicke, "Aerodynamic design studies of a transonic centrifugal compressor impeller based on automated 3D-CFD optimization," 10th Eur. Conf. Turbomach. Fluid Dyn. Thermodyn. ETC 2013, pp. 809–819, (2014)
5. Benini, E., "Three-Dimensional Multi-Objective Design Optimization of a Transonic Compressor Rotor," Journal of Propulsion and Power, Vol. 20, No. 3(2004)
6. Samad, A. and Kim, K. Y., "Application of Surrogate Modeling to Design of a Compressor Blade to Optimize Stacking and Thickness," International Journal of Fluid Machinery and Systems, Vol. 2, No. 1, pp. 1-12(2009).
7. G. A. Faza, "Multi-objective kriging-based optimization for modern wind turbine design," bachelor's thesis, Institut Teknologi Bandung, (2018).
8. C. A. Putra, "Study of multi-objective optimization of transonic compressor blade," bachelor's Thesis, Institut Teknologi Bandung, (2017).
9. G. Eisenlohr, H. Krain, F.-A. Richter, and V. Tiede, "Investigations of the flow through a high-pressure ratio centrifugal impeller," in ASME Turbo Expo 2002: Power for Land, Sea, and Air. American Society of Mechanical Engineers Digital Collection, pp. 649–657 (2002).
10. G. Eisenlohr, P. Dalbert, H. Krain, H. Pr¨oll, F.-A. Richter, and K.-H. Rohne, "Analysis of the transonic flow at the inlet of a high-pressure ratio centrifugal impeller," in Turbo Expo: Power for Land, Sea, and Air, vol. 78620. Citeseer, (1998)
11. P. W. P and F. P., Gas Turbine Performance, Oxford: Blackwell Science, (2004)
12. Casey, M. Computational geometry for the blades and internal flow channels of centrifugal compressors. In Proceedings of the ASME 1982 International Gas Turbine Conference and Exhibit, London (1982).
13. Alexander I. J. Forrester, András Sóbester, and Andy J. Keane. Engineering Design via Surrogate Modelling: A Practical Guide. 1st ed. John Wiley & Sons Ltd. ISBN: 978-0-470-06068-1(2008).
14. "Halton sequence,". [Online]. Available: https://en.wikipedia.org/ wiki/Halton sequence, last accessed,2023/07/01.
15. Yang, K., Michael E., Andre D., Thomas, B. "Multi-Objective Bayesian Global Optimization using expected hypervolume improvement gradient", in Swarm and Evolutionary Computation 44, 945–956, (2019).
16. X. He and X. Zheng, "Performance improvement of transonic centrifugal compressors by optimization of complex three-dimensional features," Proceedings of the Institution of Mechanical Engineers, Part G: Journal of Aerospace Engineering, vol. 231, no. 14, pp. 2723–2738, (2017).